

NOTES AND CORRESPONDENCE

Comments on "Inertial Instability and Mesoscale Convective Systems. Part I"

KERRY A. EMANUEL

Center for Meteorology and Physical Oceanography, Massachusetts Institute of Technology, Cambridge, MA 02139

16 October 1984

1. Introduction

An error in the linear stability analysis presented in Emanuel (1979) (hereafter referred to as "I") has been drawn to the attention of the author by Steven Meacham, currently a postdoctoral associate at MIT. The error, which pertains to the case of no-slip boundaries only, affects principally the critical shear parameter and wavelength of the instability. In this comment, we present numerically derived solutions for the critical shears and associated wavelengths and eigenmodes when no-slip boundaries are present.

2. Numerical solutions of the linear eigenvalue problem

The source of the error is in the derivation of the no-slip boundary conditions on the streamfunction (28) in I. These conditions had been derived from (25) and (26), which in turn are integrals of various combinations of the original linear equations. It is argued in I that the two integration constants that appear in the derivations of (25) and (26) must vanish in order to exclude an arbitrary geostrophic solution of the same form as the basic flow. In one case, however, the integration constant may be a function of z alone and it is not possible to prove that it must vanish under general circumstances. Under steady conditions, the boundary conditions may be expressed in terms of integrals of the streamfunction, which show that the no-slip conditions are Prandtl number-dependent. We conclude that the last two conditions (28) in I are in error.

In order to find correct solutions, we turn to a simple numerical solution of the linear equations for zonal vorticity, zonal velocity and buoyancy. We start with the hydrostatic form of the adiabatic Bousinesq primitive equations for two-dimensional perturbations to a geostrophic zonal flow that varies with y and z only, as given by (1)–(5) of I:

$$\left(\frac{\partial}{\partial t} - \nu \frac{\partial^2}{\partial z^2}\right) u' = \bar{\eta} v' - \bar{U}_z w', \quad (1)$$

$$\left(\frac{\partial}{\partial t} - \nu \frac{\partial^2}{\partial z^2}\right) v' = -\frac{1}{\rho_0} \frac{\partial p'}{\partial y} - f u', \quad (2)$$

$$\frac{1}{\rho_0} \frac{\partial p'}{\partial z} = -\frac{\rho'}{\rho_0} g, \quad (3)$$

$$\left(\frac{\partial}{\partial t} - \kappa \frac{\partial^2}{\partial z^2}\right) \frac{\rho'}{\rho_0} = -\frac{f \bar{U}_z}{g} v' + \frac{N^2}{g} w', \quad (4)$$

$$\frac{\partial v'}{\partial y} + \frac{\partial w'}{\partial z} = 0, \quad (5)$$

where the notation is the same as in I. Next we define a streamfunction ψ such that

$$v' \equiv -\frac{\partial \psi}{\partial z}, \quad w' \equiv \frac{\partial \psi}{\partial y},$$

and a buoyancy B

$$B \equiv -g \frac{\rho'}{\rho_0}.$$

Using these notations and eliminating pressure between (2) and (3) there results

$$\left(\frac{\partial}{\partial t} - \nu \frac{\partial^2}{\partial z^2}\right) u' = -\bar{\eta} \frac{\partial \psi}{\partial z} - \bar{U}_z \frac{\partial \psi}{\partial y}, \quad (6)$$

$$\left(\frac{\partial}{\partial t} - \nu \frac{\partial^2}{\partial z^2}\right) \frac{\partial^2 \psi}{\partial z^2} = f \frac{\partial u'}{\partial z} + \frac{\partial B}{\partial y}, \quad (7)$$

$$\left(\frac{\partial}{\partial t} - \kappa \frac{\partial^2}{\partial z^2}\right) B = -f \bar{U}_z \frac{\partial \psi}{\partial z} - N^2 \frac{\partial \psi}{\partial y}, \quad (8)$$

where the primes have been dropped for convenience.

We next nondimensionalize the dependent and independent variables as follows:

$$z^* \equiv H z,$$

$$y^* \equiv H \frac{N^2 \sigma}{f \bar{U}_z (1 + \sigma)} y,$$

$$t^* \equiv \frac{H^2}{\nu} t,$$

$$\psi^* \equiv f H^2 \psi,$$

$$u^* \equiv \frac{\bar{\eta} f H^3}{\nu} u,$$

$$B^* \equiv \frac{f^2 \bar{U}_z H^3}{\kappa} B,$$

where the asterisks denote dimensional variables and σ is the Prandtl number ν/κ . We also assume periodic behavior in y , seeking solutions of the form e^{ily} . With these substitutions, (6)–(8) become

$$\frac{\partial u}{\partial t} = -\frac{\partial \psi}{\partial z} - il \frac{\chi}{1 + \sigma} \psi + \frac{\partial^2 u}{\partial z^2}, \quad (9)$$

$$\frac{\partial}{\partial t} \frac{\partial^2 \psi}{\partial z^2} = T^{-1} \frac{\partial u}{\partial z} + il \chi T^{-1} \frac{\sigma}{1 + \sigma} B + \frac{\partial^4 \psi}{\partial z^4}, \quad (10)$$

$$\sigma \frac{\partial B}{\partial t} = -\frac{\partial \psi}{\partial z} - il(1 + 1/\sigma)\psi + \frac{\partial^2 B}{\partial z^2}. \quad (11)$$

The parameters which appear here are an inverse Taylor number T , a shear parameter χ , and a Prandtl number σ ; all of these are defined in I.

The above set of equations are solved numerically as an initial value problem, subject to the no-slip heat conducting boundary conditions

$$\psi = \frac{\partial \psi}{\partial z} = u = B = 0 \quad \text{on } z = 0, 1.$$

The integrations are started using the analytic inviscid-limit solutions discussed in I and carried forward in time far enough to ascertain whether the perturbation kinetic energy is increasing or decreasing with time. The integration scheme is straightforward, using leap-frog time integration (with smoothing every ten time steps) and centered second-order differencing in z . The viscous terms are lagged one time step for stability.

In order to determine the critical shear, integrations were carried out for different values of χ until approximately steady solutions were found. This was repeated for different values of the wavenumber l until the minimum value of χ was obtained. In this way, we determined the critical value of χ and the wavenumber characterizing the onset of instability.

In the case of free-slip boundaries, the boundary conditions may be expressed as homogeneous conditions on ψ and some of its vertical derivatives alone (see I). Moreover, if B and u are eliminated from the time-independent form of the set (9)–(11), the resulting equation for ψ may be reduced to sixth-order and the only parameters which appear in the equation are χ and T . Therefore, the critical value of χ is not a function of the Prandtl number σ (the Prandtl number dependence of the critical Richardson number is contained in the definition of χ). When no-slip boundaries are present, however, it is no longer possible to express the boundary conditions as homogeneous conditions on ψ and some of its vertical derivatives alone. It is, however, still possible to reduce the time-independent form of (9)–(11) to a single sixth-order equation for ψ , as shown in I. Four of the boundary conditions are homogeneous: $\psi = d\psi/dz = 0$ on $z = 0, 1$. The other two may be expressed as integrals of ψ itself. Integrating the time-

independent form of (9) between the boundaries, there results

$$il \frac{\chi}{1 + \sigma} \int_0^1 \psi dz = \frac{du}{dz} \Big|_0^1, \quad (12)$$

while merely evaluating the time-independent form of (10) at $z = 0$ and $z = 1$ results in the relation

$$\frac{du}{dz} \Big|_0^1 = -T \frac{d^4 \psi}{dz^4} \Big|_0^1, \quad (13)$$

since B vanishes on the boundaries. Eliminating the quantity $\frac{du}{dz} \Big|_0^1$ between (12) and (13), we obtain

$$il \frac{\chi}{1 + \sigma} \int_0^1 \psi dz = -T \frac{d^4 \psi}{dz^4} \Big|_0^1. \quad (14)$$

Similarly, if we integrate the time-independent form of (11) once, there results

$$il(1 + 1/\sigma) \int_0^1 \psi dz = \frac{dB}{dz} \Big|_0^1, \quad (15)$$

while evaluating the first derivative of the time-independent form of (10) with respect to z at $z = 0$ and $z = 1$ results in the relation

$$il \chi \frac{\sigma}{1 + \sigma} \frac{dB}{dz} \Big|_0^1 = -T \frac{d^5 \psi}{dz^5} \Big|_0^1, \quad (16)$$

since, from (9), $d^2 u/dz^2$ vanishes on the boundaries. Eliminating the quantity $dB/dz \Big|_0^1$ between (15) and (16), we obtain

$$l^2 \chi \int_0^1 \psi dz = T \frac{d^5 \psi}{dz^5} \Big|_0^1. \quad (17)$$

The relations (14) and (17) may be considered the remaining two boundary conditions on ψ . But note that (14) retains a Prandtl number dependence, so that in contrast to the free-slip case, *the critical value of χ will be dependent on σ when no-slip boundaries are present.*

This Prandtl number dependence is verified in the time integrations, although it appears to be quite weak for reasonable values of T . *Under no conditions was an oscillatory instability observed*; after the transients died away the time dependence always took the form of exponential growth or decay. This supports the conclusions reached by McIntyre (1970) regarding viscous symmetric instability in an unbounded fluid.

The critical value of χ , minimized with respect to wavenumber, is shown for $\sigma = 1$ as a function of T in Fig. 1, which replaces Fig. 3 of I. There is a range of T extending from 0 to about 5×10^{-4} where the critical shear for no-slip boundaries is actually smaller than that associated with free-slip boundaries; for greater viscosity, the critical shear is larger for no-slip than for free-slip boundaries. This nicely parallels the

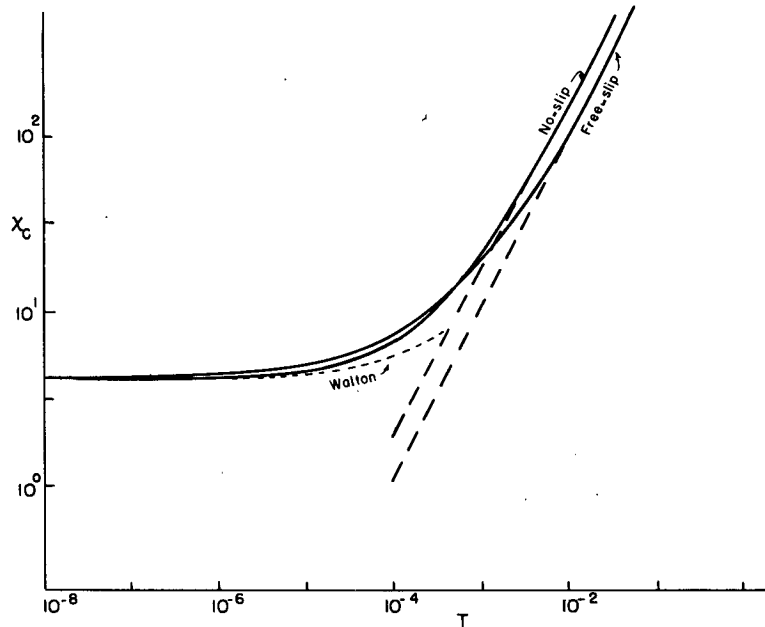


FIG. 1. The critical value of the shear parameter χ as a function of the viscous parameter T for free-slip and no-slip boundaries. Straight dashed lines are asymptotic solutions for large T ; asymptotic solution for small T by Walton (1975) also depicted. No-slip results pertain only to the case $\sigma = 1$.

solutions for the critical Rayleigh number in rotating Benard convection. When the diffusion is sufficiently small, the boundary dissipation actually assists the instability by reducing the inertial stability of the horizontal inflow and outflow branches of the circulation.

For large T , χ becomes linearly proportional to T , as explained in I. For no-slip boundaries, the relationship is approximately

$$\lim_{T \rightarrow \infty} \chi = 17\,800T$$

when $l \approx 1.4$. This should be compared with the free-slip asymptotic solution for large T from I:

$$\lim_{T \rightarrow \infty} \chi = 10\,950T$$

when $l \approx 0.838$. We see that, in contrast to the results of I, the critical value of χ for no-slip boundaries is substantially greater than the value associated with free-slip boundaries at large T .

The wavelength $L (=2\pi/l)$ associated with the onset of instability when $\sigma = 1$ is shown as a function of T in Fig. 2, which replaces Fig. 5 of I. The wavelength is actually larger for the no-slip case when T is relatively small, but becomes smaller than the free-slip wavelength at large T . This again reflects the competing effects of greater dissipation and less inertial stability along no-slip boundaries.

I have performed some experiments that demonstrate that the critical value of χ when no-slip boundaries are present does indeed depend upon the Prandtl number, although the dependence is weak. Table 1 shows the critical value of χ and the wavelength at the onset of instability for various values of σ when

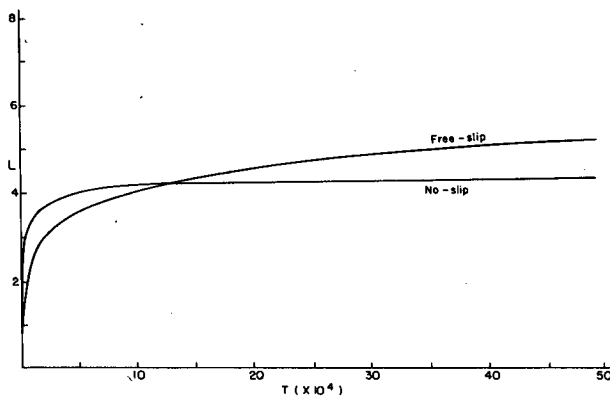


FIG. 2. Nondimensional wavelength associated with the onset of instability, as a function of T . No-slip solution pertains to the case $\sigma = 1$. Note that scale is different from Fig. 5 of I.

TABLE 1. Critical value of χ for $T = 10^{-4}$ and various Prandtl numbers.

σ	χ_c	L_c
0.2	7.58	3.30
1	6.75	3.30
3	7.16	3.25
5	7.58	3.1
10	8.17	2.9

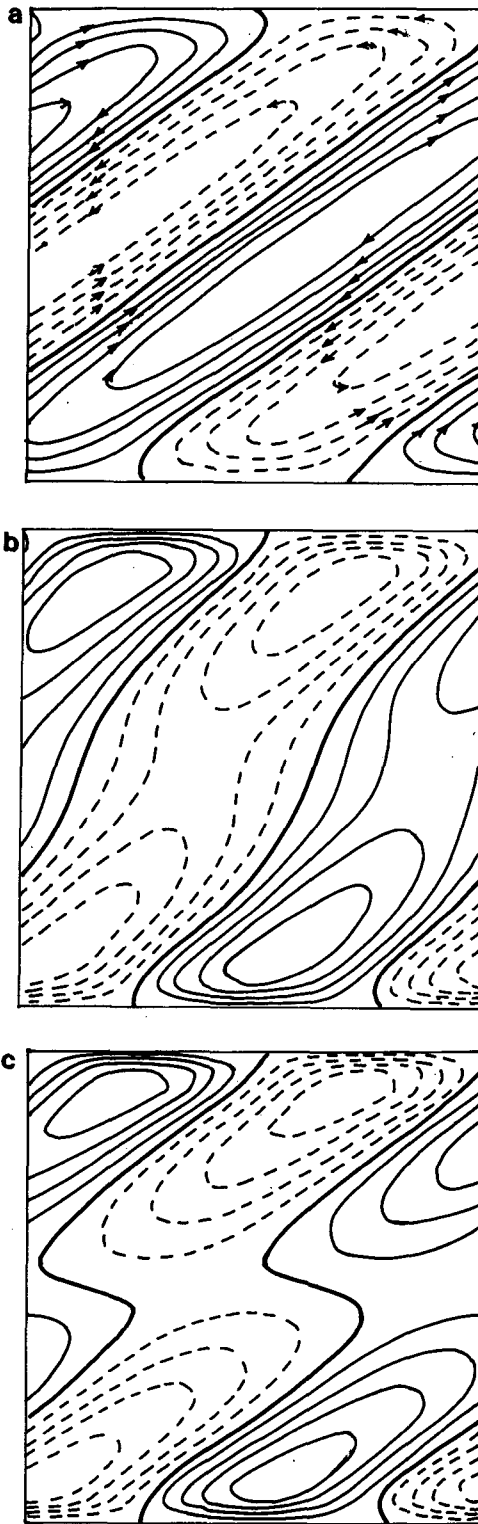


FIG. 3. (a) Streamfunction characterizing the onset of instability for no-slip boundaries, $\sigma = 1$, and $T = 10^{-6}$. One full wavelength is shown. Y increases to the right. (b) As in (a), but for zonal velocity perturbation. The amplitude of the perturbation is 0.0208 times the streamfunction amplitude. (c) As in (a), but for buoyancy perturbation. Relative amplitude is 0.0182.

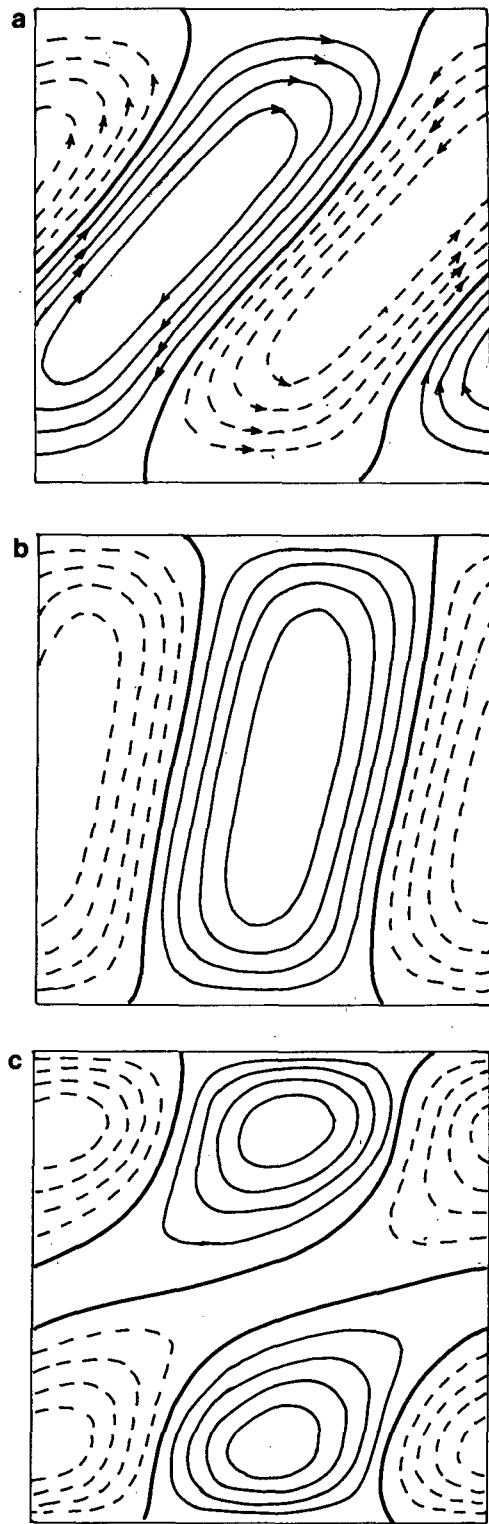


FIG. 4. (a) As in Fig. 3a, but for $T = 10^{-4}$. (b) As in Fig. 3b but for $T = 10^{-4}$. Relative amplitude is 0.1675. (c) As in Fig. 3c but for $T = 10^{-4}$. Relative amplitude is 0.055.

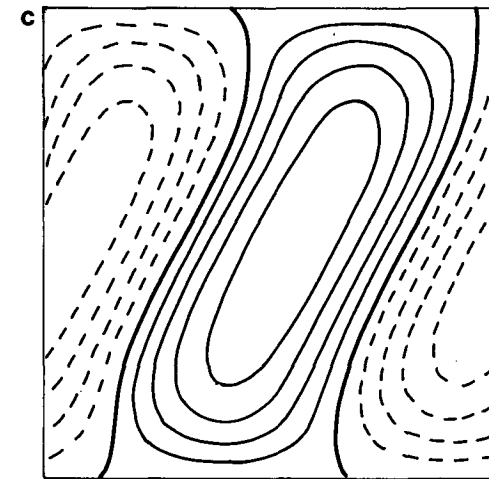
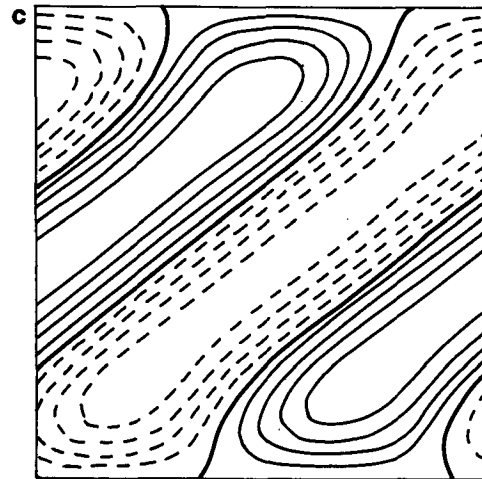
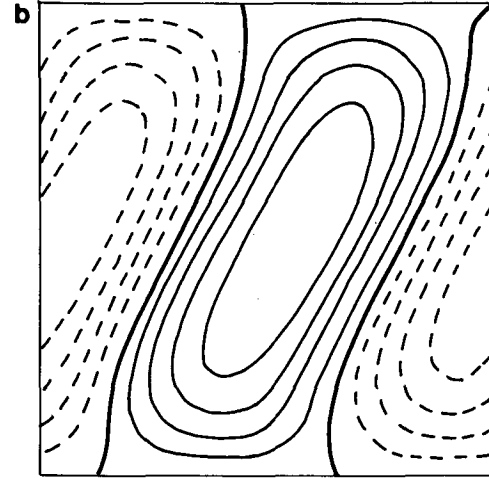
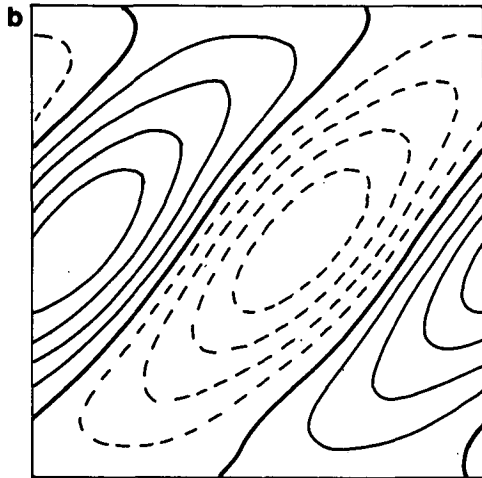
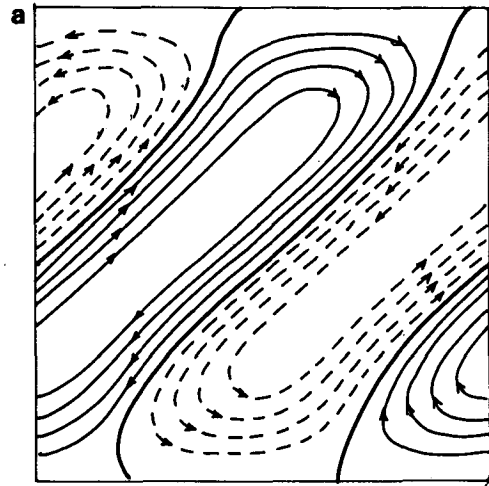
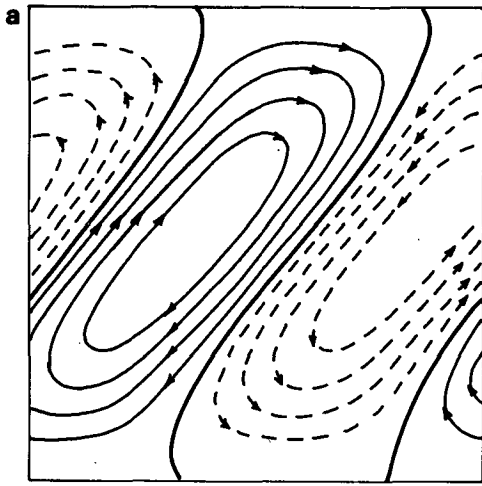


FIG. 5. (a) As in Fig. 4a, but for $\sigma = 10$. (b) As in Fig. 4b but for $\sigma = 10$. Relative amplitude = 0.099. (c) As in Fig. 4c but for $\sigma = 10$. Relative amplitude = 0.0455.

FIG. 6. (a) As in Fig. 4a, but for $\sigma = 0.2$. (b) As in Fig. 4b but for $\sigma = 0.2$. Relative amplitude = 0.3102. (c) As in Fig. 4c but for $\sigma = 0.2$. Relative amplitude = 0.2797.

$T = 10^{-4}$. It appears that the minimum χ occurs close to (if not at) $\sigma = 1$, with slightly larger values at very small and very large σ . Although this demonstrates a Prandtl number dependence, I leave a complete documentation of this effect to later work.

Finally, it is instructive to examine the form of the solutions for ψ , u and B . Figure 3 shows these fields for $\sigma = 1$ and $T = 10^{-6}$. Note that there is clearly a negative correlation between u and w , so that the disturbances convert mean zonal to disturbance kinetic energy. Most of the temperature perturbations occur near the boundaries due to horizontal temperature advection; in the interior the flow is nearly along isentropic surfaces so that temperature perturbations there are very weak. Due to the slope of the disturbances, there are regions where the static stability perturbation is strongly negative. In these regions, one might expect a slow increase in the slope of the perturbations with time, ultimately resulting in more or less upright convection.

Figure 4 is identical to Fig. 3, except that $T = 10^{-4}$. Here the only qualitative difference is that the zonal velocity perturbations have retreated into the interior. Figure 5 is for conditions identical to those shown in Fig. 4, except that here the Prandtl number is 10. Here we find remarkable differences: there are clearly positive correlations of both u and w and B and w . These disturbances thus have totally different energetics from the $\sigma = 1$ case in that kinetic energy is lost to, and available potential energy extracted from, the mean flow. Likewise, Fig. 6 (for $\sigma = 0.2$) demonstrates that the reverse is true when $\sigma < 1$; i.e., the disturbances extract kinetic energy from and give up potential energy to the mean flow. This strong dependence of the disturbance energetics on σ was discovered by Miller (1985) and has important implications for the effect of symmetric instability on

the mean flow. The reader is referred to Miller's (1985) paper for a detailed discussion of this point.

3. Conclusions

The correct solutions for the onset of symmetric instability in a viscous fluid when no-slip boundaries are present have been obtained numerically. They show that the critical value of the zonal shear is *smaller* for no-slip than for free-slip boundaries, provided that the viscosity is smaller than a critical value, while for very viscous flow the reverse is true. This is qualitatively similar to the Rayleigh convection solutions in a rotating fluid. In contrast to the case of free-slip boundaries, the critical value of χ is weakly dependent on the Prandtl number when no-slip boundaries are present. The time integrations do not show any indication that oscillatory instability is preferred under any conditions. Finally, an examination of the structure of the streamfunction, zonal velocity and buoyancy fields shows that for sufficiently large Prandtl number, symmetric instability derives energy from the mean state potential energy and gives up kinetic energy to the mean flow, in contrast to the case in which the Prandtl is smaller than or equal to 1. A full description of this interesting aspect of the energetics of symmetric instability may be found in Miller (1985).

REFERENCES

- Emanuel, K. A., 1979: Inertial instability and mesoscale convective systems. Part I: Linear theory of inertial instability in rotating viscous fluids. *J. Atmos. Sci.*, **36**, 2425-2449.
- McIntyre, M. E., 1970: Diffusive destabilization of the baroclinic circular vortex. *Geophys. Fluid Dyn.*, **1**, 19-58.
- Miller, T. L., 1985: On the energetics and nonhydrostatic aspects of symmetric baroclinic instability. *J. Atmos. Sci.*, **42**, 203-211.
- Walton, I. C., 1975: The viscous nonlinear symmetric baroclinic instability of a zonal shear flow. *J. Fluid Mech.*, **68**, 757-768.